Biogeosciences, 11, 5269–5283, 2014
www.biogeosciences.net/11/5269/2014/
doi:10.5194/bg-11-5269-2014


Biogeosciences Open Access

# Declining ozone exposure of European vegetation under climate change and reduced precursor emissions

**J. Klingberg[1,*], M. Engardt[2], P. E. Karlsson[3], J. Langner[2], and H. Pleijel[1]**

[1]Department of Biological and Environmental Sciences, University of Gothenburg, P.O. Box 461, 40530 Gothenburg, Sweden
[2]Swedish Meteorological and Hydrological Institute, 60176 Norrköping, Sweden
[3]Swedish Environmental Research Institute, P.O. Box 53021, 40014 Gothenburg, Sweden
[*]now at: Department of Earth Sciences, University of Gothenburg, P.O. Box 460, 40530 Gothenburg, Sweden

*Correspondence to:* J. Klingberg (jenny.klingberg@gvc.gu.se)

Received: 16 December 2013 – Published in Biogeosciences Discuss.: 9 January 2014
Revised: 29 August 2014 – Accepted: 29 August 2014 – Published: 1 October 2014

**Abstract.** The impacts of changes in ozone precursor emissions as well as climate change on the future ozone exposure of the vegetation in Europe were investigated. The ozone exposure is expressed as AOT40 (Accumulated exposure Over a Threshold of 40 ppb $O_3$) as well as $POD_Y$ (Phytotoxic Ozone Dose above a threshold $Y$). A new method is suggested to express how the length of the period during the year when coniferous and evergreen trees are sensitive to ozone might be affected by climate change. Ozone precursor emission changes from the RCP4.5 scenario were combined with climate simulations based on the IPCC SRES A1B scenario and used as input to the Eulerian Chemistry Transport Model MATCH from which projections of ozone concentrations were derived. The ozone exposure of vegetation over Europe expressed as AOT40 was projected to be substantially reduced between the periods 1990–2009 and 2040–2059 to levels which are well below critical levels used for vegetation in the EU directive 2008/50/EC as well as for crops and forests used in the LRTAP convention, despite that the future climate resulted in prolonged yearly ozone sensitive periods. The reduction in AOT40 was mainly driven by the emission reductions, not changes in the climate. For the toxicologically more relevant $POD_1$ index the projected reductions were smaller, but still significant. The values for $POD_1$ for the time period 2040–2059 were not projected to decrease to levels which are below critical levels for forest trees, represented by Norway spruce. This study shows that substantial reductions of ozone precursor emissions have the potential to strongly reduce the future risk for ozone effects on the European vegetation, even if concurrent climate change promotes ozone formation.

## 1 Introduction

Surface ozone ($O_3$) is the most important gaseous air pollutant with respect to effects on vegetation on regional and global scales (Hollaway et al., 2012; Mills et al., 2011; Royal Society, 2008). Experiments in which ambient $O_3$ concentrations were reduced by air filtration have shown that current levels of $O_3$ are sufficient to cause significant yield loss in sensitive crops such as wheat (Pleijel, 2011). In addition, $O_3$ affects forest growth (Braun et al., 1999, 2007; Karlsson et al., 2006), human health (Royal Society, 2008), and acts, directly and indirectly by affecting carbon storage, as an important greenhouse gas (Sitch et al., 2007).

$O_3$ is formed in the troposphere in reactions driven by the energy of solar radiation, involving the precursors nitrogen oxides ($NO_x$), volatile organic compounds (VOC) and carbon monoxide (CO). The concentration of surface $O_3$ is affected by a number of factors including (1) concentrations of $O_3$ precursors, which are a function of anthropogenic emissions and the mixing and transport in the atmosphere, (2) effects of temperature and solar radiation on the rate of chemical reactions and on emissions of biogenic VOCs, which may enhance $O_3$ formation (Doherty et al., 2013) and (3) deposition to vegetated and non-vegetated surfaces, which depends on both vertical air mixing (Klingberg et al., 2012) and the effects of air and soil humidity, solar radiation and temperature on vegetation gas exchange (Tuovinen et al., 2009).

AOT40 (the Accumulated exposure Over a Threshold of 40 ppb(v) $O_3$) has been used widely in air pollution regulation in Europe (Fuhrer et al., 1997; Mills et al., 2007; EU directive 2008/50/EC) to assess the risk of $O_3$ effects on vegetation. However, the stomatal conductance ($g_{sto}$) of plants is of critical importance for the uptake of $O_3$ and thus for its negative effects on e.g. photosynthesis (Wittig et al., 2009) and leaf senescence (Uddling et al., 2006). For example, dry air and low soil moisture tend to cause stomatal closure of plant leaves, thus reducing plant water loss and at the same time limiting plant stomatal uptake of $O_3$ (Emberson et al., 2000b; Pleijel et al., 2007). It is therefore important to consider factors influencing the stomatal uptake of $O_3$ in risk assessment (Klingberg et al., 2011). A flux-based index ($POD_Y$, phytotoxic $O_3$ dose above a flux threshold $Y$) has been developed, which takes into account the influence of temperature, solar radiation, water vapour pressure deficit (VPD), soil water potential (SWP), atmospheric $O_3$ concentration and plant development stage (phenology) on stomatal $O_3$ uptake (CLRTAP, 2011; Pleijel et al., 2007).

Several investigations have shown that climate change is likely to enhance $O_3$ formation over Europe (Demuzere et al., 2009), more so in the south than in the north (Andersson and Engardt, 2010). These earlier studies assumed constant $O_3$ precursor emissions. However, air pollutant emissions in Europe are likely to decline, both as a result of existing international legislation and as an indirect effect of attempts to reduce carbon dioxide emissions (Rafaj et al., 2013). It is difficult to estimate the development of $O_3$ precursor emissions during the present century, since it depends on e.g. political decisions that are not known. To handle this problem, four so-called RCP (Representative Concentration Pathway) scenarios have been defined to represent different possible developments of global emissions of greenhouse gases and other air pollutants (Moss et al., 2010). Using air pollutant emissions from RCP4.5, the second most optimistic RCP scenario (Thomson et al., 2011), Langner et al. (2012a) showed that this emission scenario has the potential to significantly reduce $O_3$ concentrations over Europe and that this effect is likely to be much larger than concurrent promotion of $O_3$ formation by climate change.

In this study, the chemical transport model MATCH (Robertson et al., 1999), with $O_3$ precursor emissions according to the RCP4.5 scenario and climate change under the IPCC SRES A1B scenario (Nakićenović et al., 2000), was used to estimate the combined influence of climate change and emission reductions on the future risk of $O_3$ effects on vegetation in Europe.

The aims of this study were as follows:

- To estimate the $O_3$ index AOT40, used to set target values for the protection of the vegetation against harmful effects of $O_3$ (EU directive 2008/50/EC) for crops (representing vegetation in general in the EU Directive) and trees in Europe today (1990–2009) and as projections for the near future (2040–2059), assuming $O_3$ precursor emission reductions following the RCP4.5 scenario and climate change under the IPCC SRES A1B scenario.
- To estimate the toxicologically more relevant flux-based $O_3$ index $POD_1$ for coniferous and evergreen forest trees during the time period 1960–2100 at five sites representing different climate regions in Europe.
- To suggest a new approach to assess the influence of climate change on the length of the time period during the year when coniferous and evergreen forest trees are sensitive to $O_3$.
- To assess the combined influence of climate change and $O_3$ precursor emissions reductions on AOT40 and $POD_1$ for coniferous and evergreen forest trees in Europe during the time period 1960–2100.

## 2 Methods

### 2.1 MATCH and RCA3 model setup

MATCH is an Eulerian, off-line, chemistry transport model (CTM). It is a flexible system aimed at describing the regional distribution of air pollution given relevant meteorology and emission data. Detailed description of the model can be found in Robertson et al. (1999) and Andersson et al. (2007). A number of recent studies have demonstrated the ability of MATCH to simulate $O_3$ concentrations over Europe when forced with meteorology from a regional climate model (see Andersson and Engardt, 2010; Engardt et al., 2009; Langner et al., 2012a, b). The present study uses the results described by Langner et al. (2012a) from their experiment "ECH_RCP4.5_BC2000". Here MATCH is forced with gridded and temporally evolving (1960–2100) air pollutant emission data from the RCP4.5 scenario (Thomson et al., 2011) while the meteorological data are taken from a dynamic downscaling of the global climate model ECHAM5 (Roeckner et al., 2006). The dynamic downscaling was performed with Rossby Centre's regional climate model (RCA3). Both studies use the regional climate simulation number 11 in Table 1 of Kjellström et al. (2011), which simulates the IPCC SRES A1B (Nakićenović et al., 2000) greenhouse gas emission scenario. RCA3 is described and evaluated in Samuelsson et al. (2011).

The reason for the apparent use of two different emission scenarios is that we base our work on the published downscaled climate projections from RCA3 that were available when this study was initiated. In terms of greenhouse gas concentrations the RCP4.5 and IPCC SRES A1B scenario are not very different in the period up to 2050, while towards the end of the century the climate change signal in

**Table 1.** Description of the 14 EMEP monitoring sites with $O_3$ observations and nearby temperature ($T$) observations included in the comparison between observations and simulations. The five stations used for $POD_1$ calculations are marked in bold.

| EMEPID | Station $O_3$ obs. | Latitude Longitude | Altitude (m a.s.l.) | $O_3$ data* | Station $T$ obs. | Latitude Longitude | Altitude (m a.s.l.) | $T$ data* |
|---|---|---|---|---|---|---|---|---|
| SE13 | Esrange | 67°53′ N 21°04′ E | 475 | 1991–2012 (21) | Esrange | 67°52′ N 21°05′ E | 328 | 1994–2009 (15) |
| FI22 | Oulanka | 66°19′ N 29°24′ E | 310 | 1990–2011 (19) | Kuusamo Kiutakongas | 66°22′ N 29°19′ E | 160 | 1990–2012 (23) |
| **SE35** | **Vindeln** | **64°15′ N 19°46′ E** | **225** | **1990–2012 (22)** | **Vindeln-Sunnansjönäs** | **64°08′ N 19°46′ E** | **237** | **1990–2011 (20)** |
| NO39 | Kårvatn | 62°47′ N 08°53′ E | 210 | 1992–2011 (20) | Sunndalsora III | 62°41′ N 08°34′ E | 33 | 1990–2008 (18) |
| **SE11** | **Vavihill** | **56°01′ N 13°09′ E** | **175** | **1990–2012 (23)** | **Munka-Ljungby** | **56°14′ N 12°59′ E** | **48** | **1990–2012 (23)** |
| DK41 | Lille Valby | 55°41′ N 12°08′ E | 10 | 1992–2009 (17) | Koebenhavn: Landbohojskolen | 55°41′ N 12°32′ E | 9 | 1990–2012 (23) |
| **GB02** | **Eskdalemuir** | **55°19′ N 03°12′ W** | **243** | **1990–2012 (22)** | **Eskdalemuir** | **55°19′ N 03°12′ W** | **242** | **1990–2012 (23)** |
| GB06 | Lough Navar | 54°27′ N 07°52′ W | 126 | 1990–2011 (17) | Ballyshannon | 54°30′ N 08°11′ W | 38 | 1990–2012 (22) |
| DE07 | Neuglobsow | 53°10′ N 13°02′ E | 62 | 1992–2010 (19) | Neuglobsow | 53°09′ N 13°02′ E | 62 | 1995–2009 (15) |
| NL10 | Vredepeel | 51°32′ N 05°51′ E | 28 | 1990–2010 (19) | Volkel | 51°40′ N 05°42′ E | 20 | 1990–2012 (23) |
| **AT02** | **Illmitz** | **47°46′ N 16°46′ E** | **117** | **1990–2010 (21)** | **Illmitz** | **47°46′ N 16°46′ E** | **117** | **1991–2011 (21)** |
| CH02 | Payerne | 46°49′ N 06°57′ E | 489 | 1990–2010 (20) | Payerne | 46°49′ N 06°57′ E | 490 | 1990–2012 (23) |
| **IT01** | **Montelibretti** | **42°06′ N 12°38′ E** | **48** | **1996–2009 (13)** | **Roma Ciampino** | **41°47′ N 12°35′ E** | **105** | **1990–2012 (23)** |
| ES07 | Viznar | 37°14′ N 3°32′ W | 1265 | 1998–2010 (13) | Granada | 37°08′ N 3°38′ W | 687 | 1990–2010 (21) |

*Within parentheses: number of years with less than 10 % missing data.

the RCP4.5 scenario is smaller than in IPCC SRES A1B (e.g. Rogel et al., 2012). For $O_3$ precursors there are however large differences between the scenarios, with RCP4.5 assuming much larger emission reductions than the IPCC SRES A1B scenario (see discussion in Wild et al., 2012). Global emissions of $NO_x$ and VOC for 2050 are 65 and 46 % larger, respectively, in IPCC SRES A1B than in RCP4.5 (Langner et al., 2012a). Aggregated over the European part of the CTM domain used in the study, the $NO_x$, VOC and CO emissions decrease by 53, 22 and 17 % respectively, from year 2000 to 2050 according to the RCP4.5 scenario (Langner et al., 2012a). Further characteristics of the climate and air pollutant emission scenarios are discussed in Langner et al. (2012a, b), who use this meteorological data set for studies of future $O_3$ concentrations across Europe.

The tracer boundary concentrations in MATCH (i.e. the global "background" $O_3$ concentrations) are varying seasonally, but remain the same for all years. The boundaries are based on observations from the margins of Europe (Andersson et al., 2007) and approximately represent the conditions in the year 2000. The horizontal domain and resolution of MATCH and RCA3 are identical; the models utilise a "rotated latitude–longitude grid" with grid-square sizes of approximately 50 km × 50 km.

The main time step in MATCH is 10 min; most results are saved as hourly averages. Hourly mean $O_3$ concentrations are available from the lowest model layer in MATCH (∼ 30 m), and downscaled to 3 m above ground at every time step to take into account the near-surface profile of $O_3$ generated by the surface uptake.

### 2.2 $O_3$ risk assessment: AOT40 and $POD_1$

AOT40 (Fuhrer et al., 1997) is given by

$$AOT40 = \sum \max\Big([O_3] - 40\text{ppb}, 0\Big)\Delta t, \qquad (1)$$

where $[O_3]$ is the 1 h mean $O_3$ concentration, expressed in ppb(v). AOT40 has been used widely in air pollution regulation in Europe (Fuhrer et al., 1997; Mills et al., 2007) to assess the risk for $O_3$ effects on vegetation and is included in the Mapping Manual of the Convention on Long-Range Transboundary Air Pollution (CLRTAP, 2011). In the EU legislation (EU directive 2008/50/EC) AOT40 is accumulated over the hours 8–20 CET from May to July. An AOT40 of 9000 ppb-hours is used as target value not to be exceeded and 3000 ppb-hours as a long-term objective to protect vegetation. CLRTAP (2011) uses an AOT40 critical level of 3000 ppb-hours for agricultural crops and 5000 ppb-hours for forest trees. For crops a 3-month (different months in different parts of Europe) accumulation period is used and for trees the growing season is set to April–September if site-specific information is not available. According to CLRTAP (2011), AOT40 is accumulated over daylight hours (global radiation > 50 W m$^{-2}$). The hourly mean $O_3$ concentrations at 3 m height from MATCH were used for the calculation of May–July AOT40 mainly relevant for crops, and $O_3$ concentrations from the lowest model layer in MATCH ($\sim$ 30 m) were used for the calculation of April–September AOT40 mainly relevant for trees.

The concept of AOT40 does only to a limited extent (through exclusion of the dark hours during which stomata are largely closed and the leaf gas exchange is small; CLRTAP, 2011) include factors that affect the phytotoxic relevant dose, i.e. the $O_3$ uptake through the stomata to the leaf interior where it can damage cell compartments sensitive to oxidative stress such as membranes (Sandelius et al., 1995). Despite the limitations the AOT40 index is still commonly used due to its simplicity and well-established dose–response relations. To reflect the risk for $O_3$ damage from a plant physiologically relevant perspective, the change in the $\mathrm{POD}_Y$ index was also estimated.

The stomatal $O_3$ flux was calculated using a multiplicative algorithm: an extension of the concepts presented by Jarvis (1976) and Emberson et al. (2000a, b). It includes functions accounting for the limiting effects of various abiotic factors on stomatal conductance, thereby regulating the $O_3$ flux into the plant leaf. The multiplicative algorithm is (CLRTAP, 2011)

$$g_{\mathrm{sto}} = g_{\mathrm{max}} \cdot f_{\mathrm{phen}} \cdot f_{\mathrm{light}} \cdot \max \left[ f_{\mathrm{min}}, (f_{\mathrm{temp}} \cdot f_{\mathrm{VPD}} \cdot f_{\mathrm{SWP}}) \right], \quad (2)$$

where $g_{\mathrm{sto}}$ is the stomatal conductance (mmol $O_3$ m$^{-2}$ sunlit projected leaf area (PLA) s$^{-1}$) and $g_{\mathrm{max}}$ is the species-specific maximum $g_{\mathrm{sto}}$. The functions $f_{\mathrm{phen}}$, $f_{\mathrm{light}}$, $f_{\mathrm{temp}}$, $f_{\mathrm{VPD}}$ and $f_{\mathrm{SWP}}$ are expressed in relative terms (taking values between 0 and 1). These functions allow for the influence of phenology and the environmental variables (solar radiation, temperature, VPD and SWP) on $g_{\mathrm{sto}}$ to be estimated.

The stomatal flux ($F_{\mathrm{st}}$) of $O_3$ to a plant leaf is calculated using a resistance analogue:

$$F_{\mathrm{st}} = C(z) \cdot \frac{1}{r_{\mathrm{b}} + r_{\mathrm{c}}} \cdot \frac{g_{\mathrm{sto}}}{g_{\mathrm{sto}} + g_{\mathrm{ext}}}. \quad (3)$$

The $O_3$ concentration at the top of the canopy (C(z)) is assumed to be a reasonable estimate of the concentration at the surface of the laminar leaf boundary layer near the sunlit upper canopy leaves. The $1/(r_{\mathrm{b}} + r_{\mathrm{c}})$ term is the deposition rate to the leaf determined by the quasi-laminar resistance ($r_{\mathrm{b}}$) and the leaf surface resistance ($r_{\mathrm{c}}$). $g_{\mathrm{sto}}/(g_{\mathrm{sto}} + g_{\mathrm{ext}})$ represents the fraction of the $O_3$ flux to the plant which is taken up through the stomata, where $1/g_{\mathrm{ext}}$ is the external leaf resistance. The POD accumulated per unit PLA above a threshold of $Y$ nmol m$^{-2}$ s$^{-1}$ was calculated as

$$\mathrm{POD}_Y = \sum \max \left( F_{\mathrm{st}} - Y, 0 \right) \Delta t. \quad (4)$$

The $\mathrm{POD}_Y$ is accumulated over a time period corresponding to the part of the growing season when the plant is considered to be sensitive to $O_3$. The threshold used for forest trees is $Y = 1$ nmol m$^{-2}$ PLA s$^{-1}$ (CLRTAP, 2011). Due to uncertainties caused by difficulties in modelling a plant-relevant SWP and the potentially large variations in soil moisture within a model grid, soil moisture was assumed not to limit $g_{\mathrm{sto}}$ (i.e. $f_{\mathrm{SWP}} = 1$). Hence, the estimates of $\mathrm{POD}_Y$ used in this study may be regarded as a “most sensitive case”, when the soil moisture is not limiting leaf $O_3$ uptake.

In this study the flux-based index $\mathrm{POD}_1$ (phytotoxic $O_3$ dose above a flux threshold $Y = 1$) was calculated off-line in a post-processing step at five sites (bold in Table 1) based on the methodology for different European climate regions representative tree species (i.e. Northern European Norway spruce at Vindeln and Vavihill, Atlantic Central European Scots pine at Eskdalemuir, Continental Central European Norway spruce at Illmitz and Mediterranean Holm oak at Montelibretti; CLRTAP, 2011).

$O_3$ and meteorological input data for the $\mathrm{POD}_1$ calculations should be valid for the height of the canopy, which is assumed to be 20 m for Norway spruce and Scots pine and 15 m for Holm oak. The hourly mean $O_3$ concentrations from the lowest model layer in MATCH ($\sim$ 30 m) were assumed to be representative for the forest canopy height. Modelled wind speed (from RCA3) at 10 m was adjusted to canopy height using the logarithmic wind law, assuming neutral stability. Canopy height wind speed was used to estimate the leaf boundary layer resistance required in the flux calculation. Modelled temperature and relative humidity (from RCA3) corresponding to 2 m had hourly temporal resolution. Incoming short-wave radiation data (W m$^{-2}$) was converted to photosynthetic photon flux density (PPFD) by multiplying with a factor of 2 (Monteith and Unsworth, 2008).

### 2.3 Growing season and $O_3$ sensitive period

For crops a fixed 3-month time window of May–July was used to assess AOT40 exposure in line with the EU directive (2008/50/EC). The May–July exposure window is mainly relevant for agricultural crops, but in the EU directive used for protection of vegetation. The CLRTAP Mapping Manual suggests a fixed 6-month time window of April–September to assess AOT40 exposure for forest trees. Furthermore, it is suggested to use a latitude and altitude model to estimate the start and end of the growing season of trees to assess $\mathrm{POD}_1$, if site-specific information on the relevant growing season does not exist (CLRTAP, 2011). In none of these methods is there a potential influence of climate change on the length of the growing season. Especially in cold–temperate climates, rising temperatures will extend the length of the growing season and thus the duration of the period during which plants can take up $O_3$. Sakalli and Simpson (2012) explored several methods to estimate the growing season of birch with the EMEP MSC-W model and showed that there is a strong need to include more realistic treatments of growing seasons in CTMs. Thus, in order to analyse whether or not a prolonged growing season due to climate change would counteract future reductions in $O_3$ concentration, it was necessary in this study to estimate the length of the time periods when trees may be regarded as sensitive to $O_3$, i.e. when leaf $O_3$ uptake occurs. The impacts of future climate change on the timing of budburst for deciduous tree species are governed not only by temperature, but also by day length (e.g. Arora and Boer, 2005). To avoid the complication associated with day length dependence, the analysis in this study was limited to evergreen tree species. Furthermore, we suggest using the more general concepts of an *ozone sensitive period* ($O_3$SP) instead of the term "growing season" used in the CLRTAP Mapping Manual.

In northern Europe the start of the $O_3$SP for trees was calculated as when the 24 h average temperature exceeded 5 °C for 5 consecutive days and the end as when the 24 h average temperature fell below 5 °C for 5 consecutive days (Tanja et al., 2003). The reason for using a separate definition for northern Europe is that winter dormancy represents an important limitation for physiological activity in this geographical region (e.g. Tanja et al., 2003; Kolari et al., 2007). In Atlantic Central, Continental Central and Mediterranean Europe we suggest a new approach of defining the time period when coniferous and evergreen trees are sensitive to $O_3$. The $O_3$SP was based on calculations of stomatal conductance (Eq. 2) where $f_{phen}$ and $f_{SWP}$ were set to 1 (never limiting). The calculated hourly stomatal conductance was summed for each day (24 h). The start (end) of the $O_3$SP was estimated as the first (last) day of the year when the daily summed $g_{sto}$ exceeded 30 % of the theoretically maximum daily summed $g_{sto}$ ($g_{max}$ summed over 24 h). A comparison with the growing season length calculated according to the latitude and altitude model in Mapping Manual (CLRTAP, 2011) showed that the use of a threshold of 20–30 % resulted in approximately the same length in $O_3$SP in present climate (1990–2009). The higher threshold, 30 %, was provisionally chosen in order to result in a clear signal of the potential climate change impacts on the $O_3$SP of European evergreen tree species. The stomatal conductance was calculated based on different parametrisations in different parts of Europe. The parametrisations used to calculate stomatal conductance were Scots pine in Atlantic Central Europe, Norway spruce in Continental Central Europe and Holm oak in Mediterranean Europe (CLRTAP, 2011). The $O_3$SP calculations described above were used for generating a proxy for growing season during current and future climate over which AOT40 was accumulated.

$POD_1$ was calculated over a fixed time period at five European sites, with the start and end of the stomatal $O_3$ accumulation period based on latitude and altitude (CLRTAP, 2011) and for the $O_3$SP defined above. At two sites, Illmitz in Continental Central Europe and Montelibretti in Mediterranean Europe, the $O_3$SP was defined differently for $POD_1$ compared to AOT40 in order to follow the CLRTAP Mapping Manual as closely as possible. At Illmitz the accumulation period was assumed to occur when the air temperatures fell within the $T_{min}$ and $T_{max}$ thresholds of the $f_{temp}$ relationship and for Montelibretti the accumulation period was year round with a fixed period of reduction in stomatal conductance during summer when soil water deficits are commonly high (CLRTAP, 2011). The definition of $O_3$SP and stomatal conductance parametrisations used at the different European regions and sites are summarised in Table S1 in the Supplement.

### 2.4 Comparison of simulations and observations

The MATCH-RCA3 performance has earlier been evaluated and shown good agreement with $O_3$ measurements in Europe. In Langner et al. (2012a) a comparison with summer observations revealed that the modelling system has a tendency to overestimate average $O_3$ concentrations by 1–7 %, but underestimate daily maximum concentrations by 2–7 %. According to Kjellström et al. (2011), the mean absolute error in temperature over land in RCA3 (ECHAM5 A1B-r3) is 0.90–1.05 °C in spring, summer and autumn.

In this study, observed $O_3$ concentrations and temperatures were used to estimate the performance of the MATCH-RCA3 modelling system at 14 monitoring sites within the European Monitoring and Evaluation Programme (EMEP) within CLRTAP. These sites were chosen since they had long time series of $O_3$ concentration observations and available nearby temperature measurements (within the same grid cell in MATCH). Hourly $O_3$ observations were obtained from the EMEP website (www.emep.int) and air temperature observations from the Swedish Meteorological and Hydrological Institute (www.smhi.se), European climate assessment and data set (Tank et al., 2002), Umweltbundesamt, Austria and the Federal Environment Agency, Germany. Only years with less than 10 % missing data were included. More information about the sites is given in Table 1 and locations are shown in Fig. 1a. The RMSE (root mean square error), spatial correlation and bias of model and observations were calculated for daily minimum, mean and maximum temperature, daily mean and maximum $O_3$ concentrations and May–July AOT40. Spatial correlation is the correlation between the 14 pairs of time-averaged observed and modelled values – 14 is the number of sites included in the comparison in this study (Table 1).

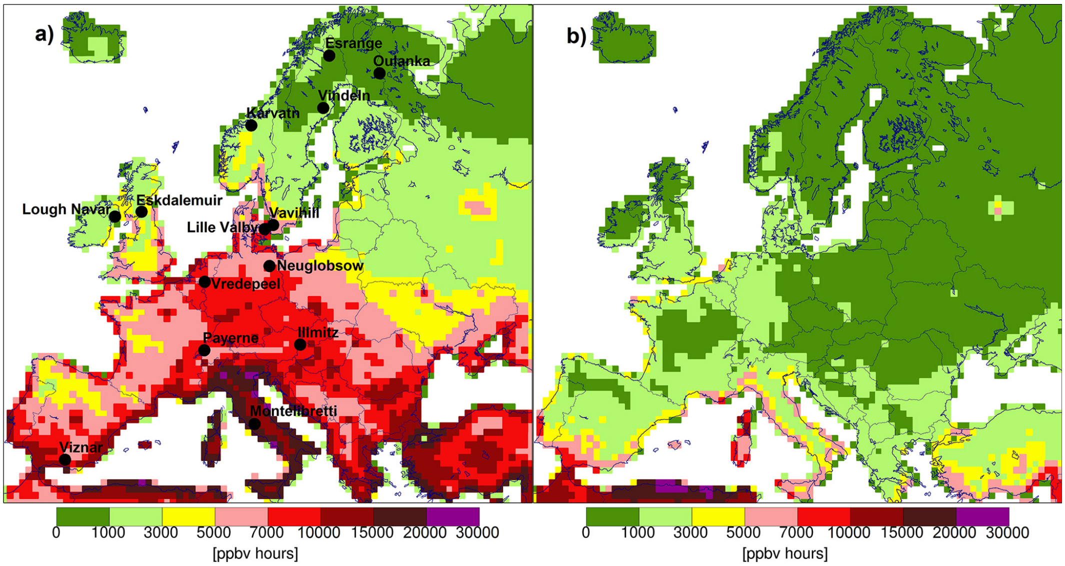


**Figure 1.** Present and future modelled AOT40 (ppb-hours) as 20-year averages, 1990–2009 **(a)** and 2040–2059 **(b)** assuming $O_3$ precursor emission reductions according to the RCP4.5 scenario and climate change under the IPCC SRES A1B scenario. AOT40 was accumulated over the hours 8–20 CET during May–July, which is used in the EU directive 2008/50/EC for protection of vegetation, but mainly relevant for crops. Model results are from 3 m above ground. Included in **(a)** are the 14 EMEP monitoring sites used for comparison between observations and model simulations (Table 1).

## 3 Results and discussion

### 3.1 Model performance

The results of the comparisons of simulations with observations are displayed in Table 2. The spatial correlation of temperature was high but the model tends to underestimate maximum temperatures by on average 2.8 °C. The daily average $O_3$ concentrations had notably low spatial correlation, which was also observed in Langner et al. (2012a) for stations north of 50° N. The May–July AOT40 was on average well captured by the model with only a small average bias of −15 %, which indicates that systematic errors in the calculations of AOT40 are likely to be minor. However, for individual sites the differences can be rather large as shown by the RMSE of 2888 ppb-hours. Regional-scale models often tend to underestimate peak $O_3$ concentrations during $O_3$ episodes (Langner et al., 2012b). This is the case also with the MATCH model in this study. As a result, modelled daily maximum $O_3$ concentrations and AOT40 are underestimated to a greater extent than modelled average $O_3$ concentrations compared to observations.

Further comparisons between observations and simulations with respect to $O_3$ concentrations and temperature at the five sites (shown in bold in Table 1) selected to illustrate differences in the evolvement of $O_3$SP, AOT40 and $POD_1$ 1960–2100 in different European climate regions are shown in Figs. S1 and S2 in the Supplement.

### 3.2 Changes in AOT40 with a fixed accumulation period

The estimated daytime (8–20 CET) AOT40 across Europe, accumulated during May–July mainly relevant for crops but representing vegetation in general in the EU directive, is shown in Fig. 1a for the period 1990–2009 and in Fig. 1b as a projection for the period 2040–2059. For the period 1990–2009, the long-term EU objective of 3000 ppb-hours (which is also the CLRTAP critical level, but note the slightly different definition of accumulation period) was exceeded over most of Europe including a large part of the UK and the southern parts of Fennoscandia. For the period 2040–2059, the projected AOT40 was estimated to exceed 3000 ppb-hours only in the Mediterranean area and at some spots along the coasts of Portugal, France, Belgium, Netherlands and the southern parts of the UK. The high levels along the coastal areas are the result of the higher $O_3$ concentrations over the sea, resulting from low deposition and the well-mixed marine boundary layer as compared to land, which also affect coastal areas (Pleijel et al., 2013).

Figure 2 shows time series of the May–July AOT40 values over the period 1960–2100 at five sites. It suggests that AOT40 peaked before 2000 and is followed by a decline until 2100. From Fig. 2 it can be inferred that by the second half of the present century, May–July AOT40 values have declined not only below the EU target value of 9000 ppb-hours but, with the exception of Montelibretti, also the long-term objective of 3000 ppb-hours based on the model results and emission scenarios used in this study. The performance of the MATCH model is indicated by the inclusion of observed data

**Table 2.** Comparison between observations and simulations of daily average, maximum and minimum temperature ($T$ in °C) over the whole year, daily average and maximum $O_3$ (ppbv) at 3 m above ground over the whole year and AOT40 accumulated from May to July (ppb-hours) of the 14 EMEP monitoring sites and nearby temperature observations described in Table 1.

| | $T_{mean}$ (°C) | $T_{max}$ (°C) | $T_{min}$ (°C) | $O_3$ mean (ppb) | $O_3$max (ppb) | AOT40mjj (ppbh) |
|---|---|---|---|---|---|---|
| RMSE | 1.6 | 3.0 | 2.3 | 4.8 | 2.7 | 2888 |
| Spatial correlation | 0.95 | 0.96 | 0.91 | 0.22 | 0.80 | 0.78 |
| Mean obs. | 8.3 | 12.7 | 4.1 | 28.3 | 39.5 | 5539 |
| Mean model | 7.6 | 9.9 | 5.4 | 29.7 | 38.6 | 4705 |
| Bias | −0.7 | −2.8 | 1.3 | 1.4 | −1.0 | −834 |

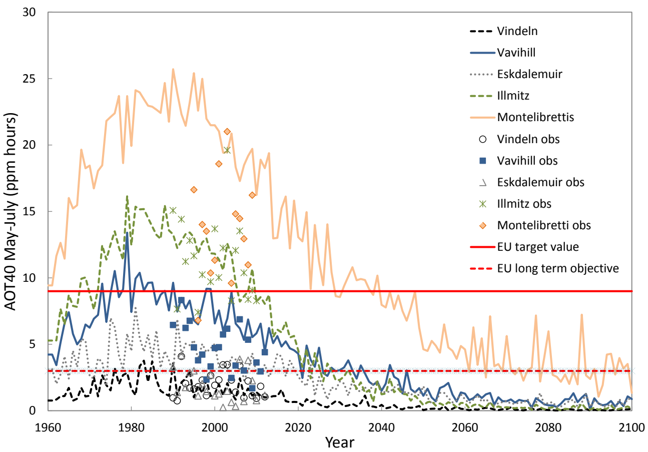


**Figure 2.** Modelled AOT40 (ppm-hours), 3 m above ground, accumulated over the hours 8–20 CET during May–July 1960–2100 at five sites in Europe assuming $O_3$ precursor emission reductions according to the RCP4.5 scenario and climate change under the IPCC SRES A1B scenario. Discrete symbols represent AOT40 based on observations of $O_3$ concentrations ∼ 1990–2012 at these sites. The May–July AOT40 is used in EU directive 2008/50/EC for protection of vegetation, but is mainly relevant for crops.

at the five sites considered. Note that observations are not directly comparable to model results from the same simulated year since MATCH is driven by meteorology from a climate model and not observed meteorology. The large between-years variation in AOT40 derived from observations was not resolved by the model. This is partly related to the underestimation of the meteorological variability in our regional climate model compared to the real world. It is also related to the general problem of calculating the accumulated sum of exceedances, close to ambient levels. Although MATCH in general underestimates AOT40 (see Table 2), the model overestimates AOT40 at Vavihill, Eskdalemuir and Montelibretti. However, the model captures the range of AOT40 from low in the north to high in the south of Europe reasonably well.

The estimated daylight (global radiation $> 50\,W\,m^{-2}$) AOT40 during the fixed April–September period mainly relevant for forest trees across Europe is shown in Fig. 3a as a mean value for the period 1990–2009 and in Fig. 3b as a projection for the period 2040–2059. The CLRTAP critical level of 5000 ppb-hours was exceeded in 1990–2009 over most of Europe, including most of the UK and the southern parts of Fennoscandia. By the period 2040–2059, the exceedance was greatly reduced and again restricted to the Mediterranean region and some coastal spots around Spain, France, Belgium, the Netherlands and the UK.

**Table 3.** Average length of the $O_3$ sensitive period ($O_3$SP in days) relevant for coniferous and evergreen tree species during the two 20-year time periods 1990–2009 and 2040–2059 at the five sites representing different climate regions of Europe.

| | Vindeln | Vavihill | Eskdalemuir | Illmitz | Montelibretti |
|---|---|---|---|---|---|
| 1990–2009 | 158 | 265 | 196 | 324 | 254 |
| 2040–2059 | 183 | 294 | 203 | 341 | 264 |
| Change | 24 | 29 | 7 | 17 | 10 |

The likelihood of the projections regarding the decline in the exceedance of AOT40 for crops and forests (Figs. 1–3) depends strongly on the achievability of the rather extensive reduction of $O_3$ precursor emissions suggested by the RPC4.5 scenario. Langner et al. (2012a) showed that even though climate change leads to increasing surface $O_3$ concentrations during April–September in some areas of Europe, the RCP4.5 projected air pollutant emission reductions in Europe have a much stronger opposing effect, resulting in net reductions of $O_3$ concentrations. Provided that the substantial air pollutant emission reductions suggested by the RCP4.5 scenario is achieved, $O_3$ concentrations will reach levels where AOT40 declines strongly and may be well below current limit values over large areas, but not the whole of Europe. The AOT40 index, which is based on the exceedance of a relatively high threshold, and thus highly sensitive to modest changes in concentrations near that threshold (Sofiev and Tuovinen, 2001), declines much more than the average $O_3$ concentrations (data not shown). Thus, AOT40 is more sensitive to emission reductions compared to concentration averages.

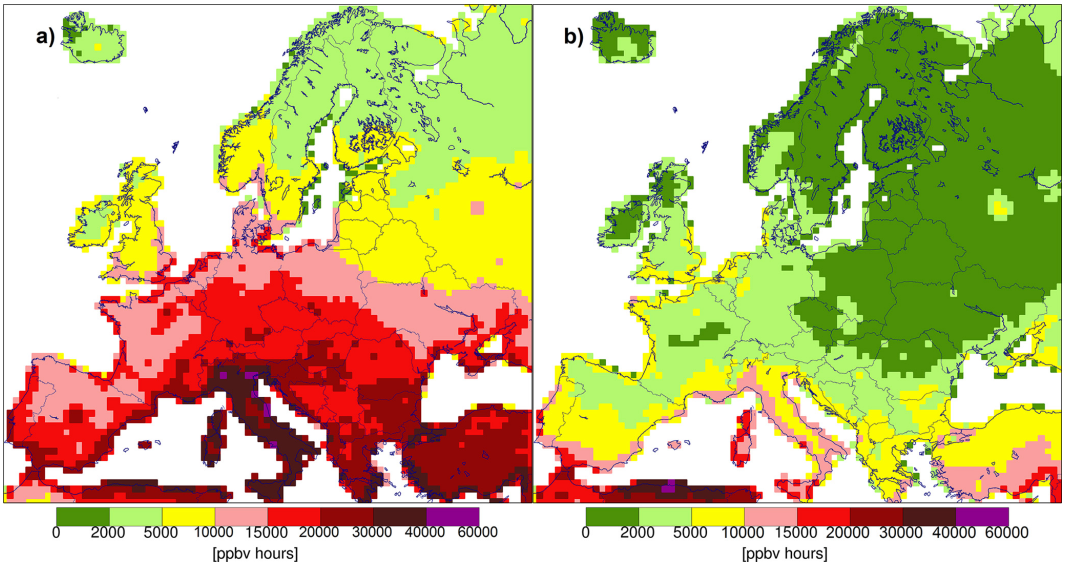


**Figure 3.** Present and future modelled AOT40 (ppb-hours) as 20-year averages **(a)** 1990–2009 and **(b)** 2040–2059 assuming $O_3$ precursor emission reductions according to the RCP4.5 scenario and climate change under the IPCC SRES A1B scenario. AOT40 was accumulated over daylight hours (global radiation $> 50\,W\,m^{-2}$) during the fixed April–September accumulation period mainly relevant for forest trees. Model results are based on $O_3$ concentrations from the lowest model layer ($\sim 30$ m above ground).

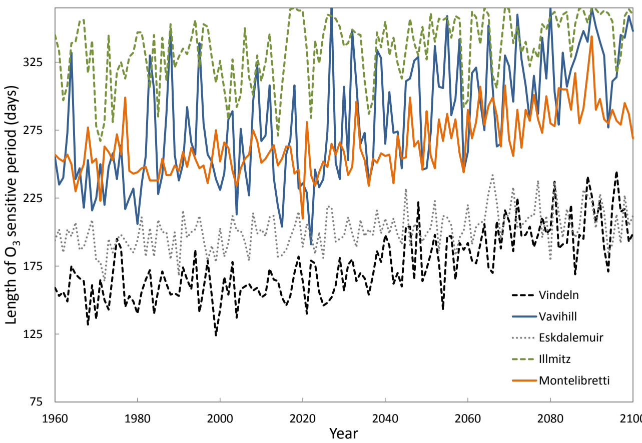


**Figure 4.** Calculated length of $O_3$ sensitive period (days), relevant for coniferous and evergreen tree species, during 1960–2100 at five sites in Europe. At Vindeln and Vavihill (Northern Europe) the start (end) of the period is defined as when the daily average temperature exceeds (falls below) 5 °C on 5 consecutive days. At Eskdalemuir (Atlantic Central Europe), Illmitz (Central Continental Europe) and Montelibretti (Mediterranean Europe) the start (end) of the period is defined as the first (last) day that the daily summed stomatal conductance exceeds 30 % of the theoretical maximum daily summed stomatal conductance. At Illmitz the stomatal conductance was calculated based on Continental Central European Norway spruce parametrisation, at Eskdalemuir the Atlantic Central European Scots pine parametrisation and at Montelibretti the Mediterranean Europe Holm oak parametrisation.

### 3.3 Changes in $O_3$ sensitive period and AOT40

In Fig. 4 the length of the $O_3$SP for trees is shown at five sites across Europe 1960–2100. The duration of the $O_3$SP for trees is projected to increase at all five sites (see also Table 3), with the most pronounced increases in northern Europe. An earlier onset of the growing season during spring is of particularly large importance in northern Europe (Karlsson et al., 2007) since the $O_3$ concentrations can be high at northern latitudes during this time of year (Klingberg et al., 2009). Today this $O_3$ peak mostly takes place before the start of the growing season, but may overlap to a larger extent with $O_3$SP in the future.

The estimated daylight AOT40 during the $O_3$SP is shown in Fig. 5a as a mean value for the period 1990–2009 and in Fig. 5b as a projection for the period 2040–2059. As a consequence of the extended $O_3$SP suggested by the model (Table 3 and Fig. 4), the period during which AOT40 was accumulated in Fig. 5b was generally longer than in Fig. 5a. The strong reduction in AOT40 between the two periods is the net effect of reduced emissions of $O_3$ precursors which act to reduce $O_3$ concentrations, and on the other hand two factors that favour an increase in $O_3$ exposure: a longer accumulation period and the promotion of $O_3$ formation by climate change. By comparing the changes in AOT40 revealed by Figs. 3 and 5, respectively, it is evident that reduced emissions of $O_3$ precursors is the dominating effect and that a prolonged accumulation period does not substantially reverse this effect. Hence, it further emphasises the strong reduction in $O_3$ exposure, resulting from the strict air pollutant emission reductions under the RCP4.5 scenario used in the model setup.

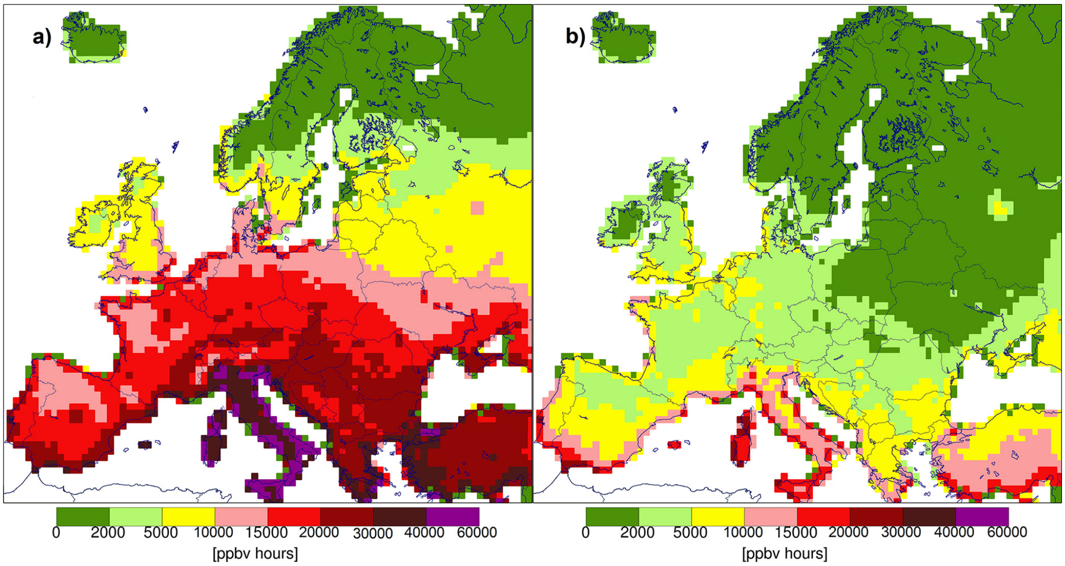


**Figure 5.** Present and future modelled AOT40 (ppb-hours) as 20-year averages **(a)** 1990–2009 and **(b)** 2040–2059 assuming $O_3$ precursor emission reductions according to the RCP4.5 scenario and climate change under the IPCC SRES A1B scenario. AOT40 was accumulated over daylight hours (global radiation $> 50\,W\,m^{-2}$) during the $O_3$ sensitive period relevant for coniferous and evergreen tree species. Model results are based on $O_3$ concentrations from the lowest model layer ($\sim 30$ m above ground)

### 3.4 Changes in $POD_1$

In Fig. 6a–e the projections for AOT40 and $POD_1$ using two different accumulation periods are compared for the sites Vindeln, Vavihill, Eskdalemuir, Illmitz and Montelibretti. Several important observations can be made from the projections. Although $POD_1$ declines at all sites (most strongly in Illmitz and Montelibretti), the decline is much smaller than the decline in AOT40. Thus the estimated improvement in terms of risk for vegetation is likely to be larger by using AOT40 rather than the physiologically and toxicologically more relevant $POD_1$. While the critical level value for AOT40 is suggested to be exceeded only and just marginally at Montelibretti by the end of this century, the critical level of the $POD_1$ index continues to be exceeded in Vavihill, Eskdalemuir, Illmitz and Montelibretti and, depending on which definition of the accumulation period is used, even at far north Vindeln.

The fact that AOT40 is declining at a much faster rate than $POD_1$ is related to the fact that concentrations as low as 10–15 ppb (data not shown) will contribute to $POD_1$ when stomatal conductance is relatively high. Thus $POD_1$ is more linked to the development of low to moderate $O_3$ concentrations, which are suggested to change much less than higher $O_3$ concentrations and the exceedance of 40 ppb defining the concept of AOT40.

$POD_1$ generally declined at a slower rate when calculated with an accumulation period based on $O_3$SP as compared to when based on the fixed accumulation period calculated from the latitude and altitude model (Fig. 6). This is partly explained by the observation (Fig. 4) that the projected future climate will increase the duration of the $O_3$SP.

To shed further light on the effect of altered climate on $g_{sto}$ and thus $O_3$ uptake as defined in $POD_1$, Fig. 7 shows the daily summed $g_{sto}$ based on modelled temperature, VPD and solar radiation as an average for the periods 1990–2009 and 2040–2059 at the five sites in Europe. Although these calculations suggest a stronger summer depression of $g_{sto}$ in Illmitz and Montelibretti, and a weak but general increase in spring and fall conductance for 2040–2059 compared to 1990–2009, the overall pattern is not suggested to change much. Thus, it can be concluded that also for $POD_1$, as earlier noted for AOT40, the major driver of the declining $POD_1$ values was reduced emissions of $O_3$ precursors.

### 3.5 Uncertainties and future work

In this study we have described how AOT40 is affected by projected $O_3$ precursor emission reductions according to the RCP4.5 scenario and climate change under the IPCC SRES A1B scenario. We have also estimated the present century change of $POD_1$ at five sites across Europe based on the same climate and air pollutant emission projections. Included in the flux-based $O_3$ index $POD_1$ were the influence of phenology and the environmental variables solar radiation, temperature and VPD on $g_{sto}$ and the risk of $O_3$ damage to vegetation.

It is important to note that this study did not include the effect of changing soil moisture. Especially in southern Europe drought is an important factor influencing the $g_{sto}$ (e.g. Paoletti, 2009, Büker et al., 2012). In part, this is taken into

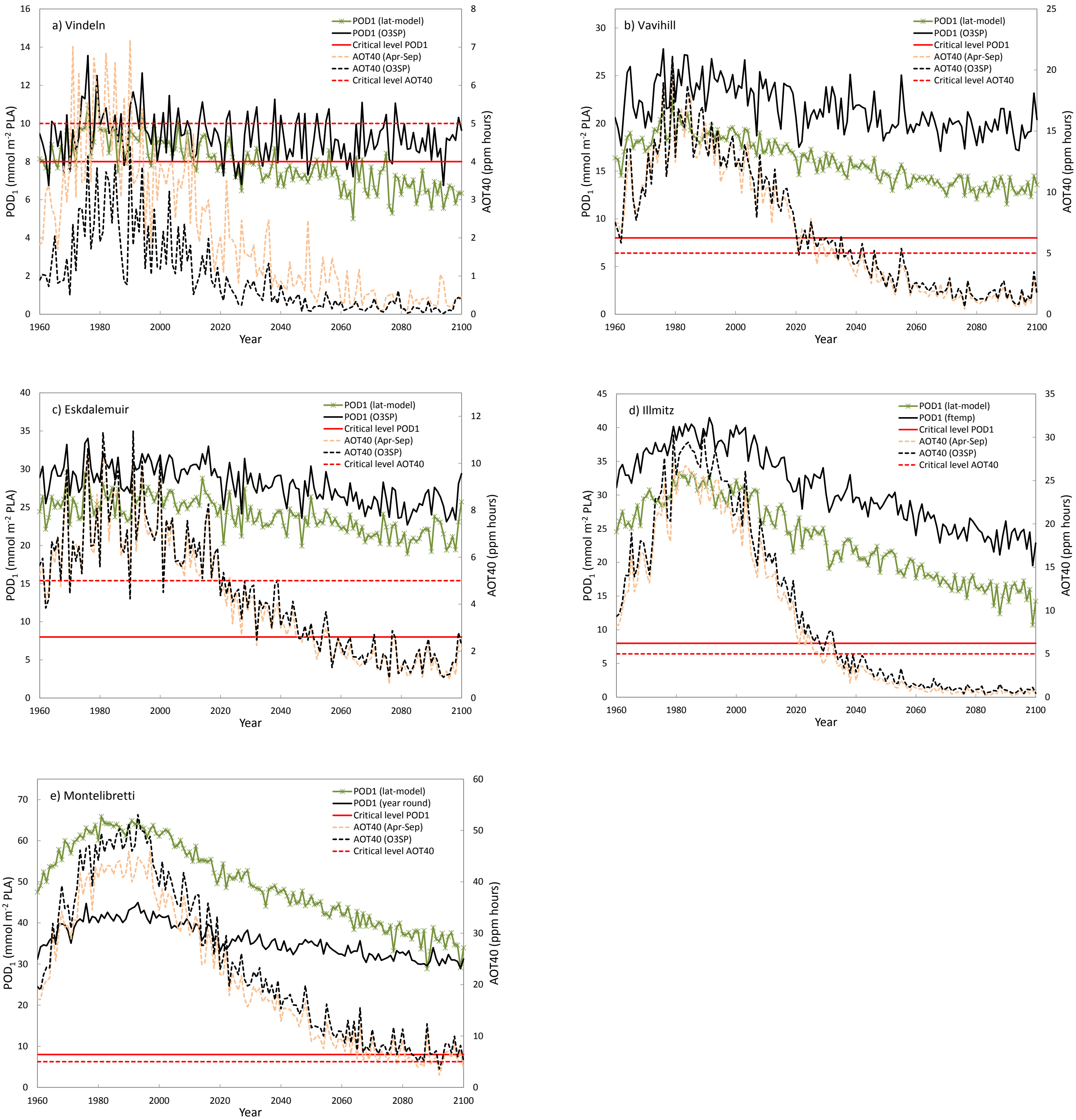


**Figure 6.** Modelled $POD_1$ and AOT40 at **(a)** Vindeln, **(b)** Vavihill, **(c)** Eskdalemuir, **(d)** Illmitz and **(e)** Montelibretti during 1960–2100. $POD_1$ was calculated based on the northern European Norway spruce parametrisation (Vindeln and Vavihill), the Atlantic Central European Scots pine parametrisation (Eskdalemuir), the Continental Central European Norway spruce parametrisation (Illmitz) and the Mediterranean Europe Holm oak parametrisation (Montelibretti). At all sites $POD_1$ and AOT40 was calculated for a fixed time period (not changing in time), for $POD_1$ based on the Mapping Manual latitude and altitude model (lat-model) and for AOT40 April–September. AOT40 and $POD_1$ were also calculated over the $O_3$ sensitive period ($O_3$SP) shown in Fig. 4. At Illmitz and Montelibretti the $O_3$SP was defined differently for $POD_1$ compared to AOT40 in order to follow the CLRTAP Mapping Manual as close as possible (see also Table S1 in the Supplement). For Illmitz the accumulation period of $POD_1$ was assumed to occur when the air temperatures fell within the $T_{min}$ and $T_{max}$ thresholds of the $f_{temp}$ relationship ($POD_1$ $f_{temp}$) and for Montelibretti the $POD_1$ accumulation period was year round with a fixed period of reduction in stomatal conductance during summer when soil water deficits are commonly high ($POD_1$ year round).

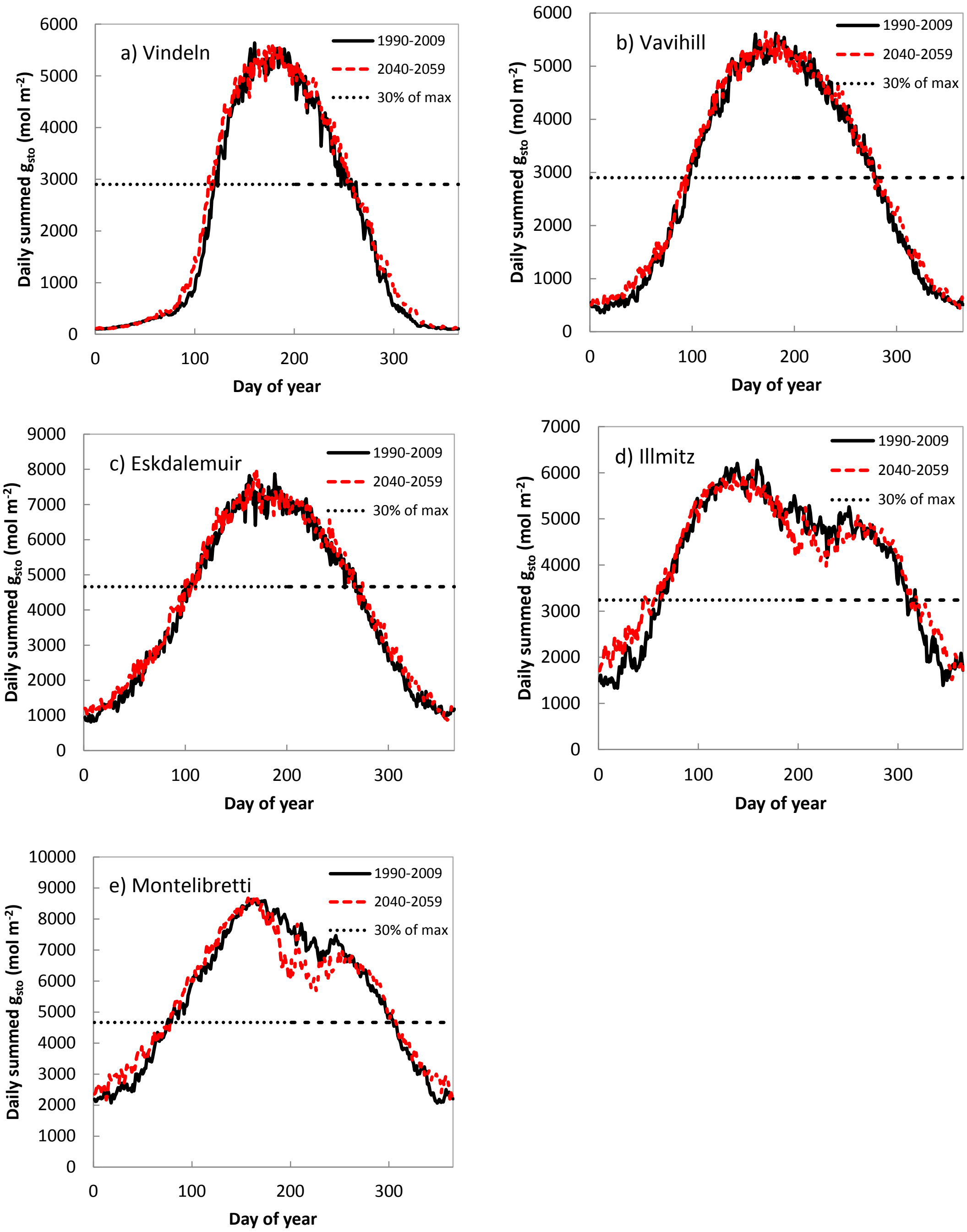


**Figure 7.** Daily summed stomatal conductance ($g_{sto}$) based on temperature, VPD and light as an average year 1990–2009 and 2040–2059. At **(a)** Vindeln and **(b)** Vavihill the stomatal conductance was calculated based on the northern European Norway spruce parametrisation, at **(c)** Eskdalemuir the Atlantic Central European Scots pine parametrisation, at **(d)** Illmitz the Continental Central European Norway spruce parametrisation and at **(e)** Montelibretti the Mediterranean Europe Holm oak parametrisation. The dotted line represents the 30 % threshold of the theoretically maximum daily summed $g_{sto}$, used to define the $O_3$ sensitive period at each site.

account through the phenology function in the calculations of $POD_1$ in Mediterranean Europe (see also Table S1 in the Supplement). This study should be regarded as a "most sensitive case", representing a situation when soil moisture is not limiting leaf $O_3$ uptake. The inclusion of soil moisture could lead to further reductions in $POD_1$ and, through a shorter $O_3$SP, also AOT40. Thus, improved modelling of soil moisture across Europe would be of great value for analyses of future $O_3$ impact on vegetation.

An additional factor with potential to significantly reduce $O_3$ toxicity, which was not taken into account in this study, is the projected reduction in stomatal conductance under rising $CO_2$ concentrations in future climate (Klingberg et al., 2011). The sensitivity of vegetation to $O_3$ would also be affected by potential future changes in land-use and changes in the composition of species. Further uncertainties lie in potential changes in antioxidative defence capacity and secondary effects such as pest and diseases (Fuhrer, 2009). These factors have not been considered in this study, but deserve further investigation.

In order to focus on the effect of climate change and decreasing European air pollutant emissions, we kept the tracer boundary concentrations of our regional CTM constant in this study. This is clearly a simplification given the substantial role of external sources to background concentrations of $O_3$ in Europe (Wild et al., 2012). Recent studies with global CTMs using climate projections and air pollutant emissions following the four RCPs (Young et al., 2013) point towards small (0–2 ppb) decreases of the $O_3$ concentration across most of the Northern Hemisphere troposphere from 2000 to 2030. In 2100 the decreases in annual mean concentrations have increased to 5–10 ppb according to these studies. These findings strengthen our conclusion that if European (and global) emissions follow the RCP4.5 pathway, $O_3$ exposure of European vegetation is likely to be reduced significantly from 2000 to 2050.

The results presented in this study strongly depend on the choice of emission scenario for $O_3$ precursors in Europe. The RCP4.5 emission scenario assumes substantial air pollution abatement measures and it remains to be seen if these reductions can be realised. According to the IIASA TSAP-2012 baseline scenario, which assumes full implementation of existing air pollution control legislation of the European Union, $NO_x$ emissions are reduced by $> 65\,\%$ and VOC emissions decline by 40 % in the EU-27 until 2030 compared to 2005 (Amann, 2012). Between 2030 and 2050 the emissions are more or less constant in that scenario. This suggests that for the first half of the century, the decline in air pollutant emissions in the RCP4.5 scenario are actually smaller than the reductions assumed if existing air pollution control legislation are implemented.

The European $O_3$ concentrations in 2050 are substantially smaller than those in the IPCC SRES A1B, A2 and B2 scenarios under all four RCP scenarios as shown by Wild et al. (2012). RCP4.5 is the second most optimistic of the RCP scenarios regarding $O_3$ precursor emission reductions. With this study we demonstrate that if substantial air pollution control measures are undertaken, it is possible to significantly reduce the negative effects of $O_3$ on vegetation in a not too distant future.

Finally, future analyses of $O_3$ effects on European vegetation would benefit from validation of the relevance of the $POD_1$ index, the dose–response functions based on $POD_1$ and the limit values used. This would require new, well-designed toxicological experiments, such as FACE (free-air $O_3$ enrichment) and chamber experiments including filtered air treatments as well as studies based on epidemiological techniques, providing independent data sets to further evaluate the current methodology for estimating the magnitude of biological effects.

## 4 Conclusions

This study considered the combined effect of projected emission reductions according to the RCP4.5 air pollutant emission scenario and climate change under the IPCC SRES A1B scenario during the period 1960–2100. The following important conclusions can be drawn:

- Powerful, but realistic, air pollutant emission reductions outlined in the RCP4.5 scenario have the potential to strongly reduce the exposure of plants to $O_3$ in Europe. Over wide areas AOT40 will, by the time period 2040–2059, decrease to levels which are well below $O_3$ critical levels used for vegetation in the EU legislation as well as critical levels used in the LRTAP convention.

- For the physiologically and toxicologically more relevant $POD_1$ index the reductions are smaller, but still substantial, especially in South and Central Europe. However, the values for $POD_1$ by the time period 2040–2059 will not decrease to levels which are below $O_3$ critical levels used for forest trees, represented by Norway spruce, in the methods currently used by LRTAP Convention.

- The smaller reductions of the $POD_1$ values are explained by the fact that this index is more sensitive to the development of low to moderate $O_3$ concentrations, while AOT40 depends strongly on the peaks of $O_3$, i.e. the time-integrated exceedance of the concentration over 40 ppb $O_3$ will decline much more than concentrations above the lower threshold (ca. 10–15 ppb) associated with $POD_1$.

- If emissions are not substantially reduced in line with the RCP4.5 scenario, surface $O_3$ will continue to be a serious problem to European vegetation, which is aggravated by climate change.

**The Supplement related to this article is available online at doi:10.5194/bg-11-5269-2014-supplement.**

*Acknowledgements.* This study was supported by the research programme CLEO (Climate Change and Environmental Objectives) funded by the Swedish Environmental Protection Agency, the strategic research area BECC (Biodiversity and Ecosystem Services in a Changing Climate) and the European Union seventh framework programme project ECLAIRE (Effects of Climate Change on Air Pollution and Response Strategies for European Ecosystems, Project No. 282910). Special thanks are due to Umweltbundesamt, Austria, who provided temperature data from Illmitz and the Federal Environment Agency – Air Monitoring Network, Germany, who provided temperature data from Neuglobsow.

Edited by: S. Zaehle

## References

Amann, M.: Future emissions of air pollutants in Europe - Current legislation baseline and the scope for further reductions, TSAP Report #1, Version 1.0, DG-Environment, European Commission, Belgium, produced under Service contract on Monitoring and Assessment of Sectorial Implementation Actions (ENV.C.3/SER/2011/0009) (available at: http://www.iiasa.ac.at/web/home/research/researchPrograms/MitigationofAirPollutionandGreenhousegases/TSAP-BASELINE-20120613.pdf), 2012.

Andersson, C. and Engardt, M.: European ozone in a future climate: Importance of changes in dry deposition and isoprene emissions, J. Geophys. Res.-Atmos., 115, D02303. doi:10.1029/2008JD011690, 2010.

Andersson, C., Langner, J., and Bergström, R.: Interannual variation and trends in air pollution over Europe due to climate variability during 1958–2001 simulated with a regional CTM coupled to the ERA40 reanalysis, Tellus B, 59, 77–98, 2007.

Arora, V. K. and Boer, G. J.: A parameterization of leaf phenology for the terrestrial ecosystem component of climate models, Glob. Change Biol., 11, 39–59, 2005.

Braun, S., Rihm, B., Schindler, C., and Fluckiger, W.: Growth of mature beech in relation to ozone and nitrogen deposition: An epidemiological approach, Water Air Soil Poll., 116, 357–364, 1999.

Braun, S., Schindler, C., Rihm, B., and Fluckiger, W.: Shoot growth of mature *Fagus sylvatica* and *Picea abies* in relation to ozone, Environ. Pollut., 146, 624–628, 2007.

Büker, P., Morrissey, T., Briolat, A., Falk, R., Simpson, D., Tuovinen, J.-P., Alonso, R., Barth, S., Baumgarten, M., Grulke, N., Karlsson, P. E., King, J., Lagergren, F., Matyssek, R., Nunn, A., Ogaya, R., Peñuelas, J., Rhea, L., Schaub, M., Uddling, J., Werner, W., and Emberson, L. D.: DO3SE modelling of soil moisture to determine ozone flux to forest trees, Atmos. Chem. Phys., 12, 5537–5562, doi:10.5194/acp-12-5537-2012, 2012.

CLRTAP: Manual on Methodologies and Criteria for Modelling and Mapping Critical Loads & Levels and Air Pollution Effects, Risks and Trends. UNECE Convention on Long-range Transboundary Air Pollution (Available and continuously updated at www.icpmapping.org), 2011.

Demuzere, M., Trigo, R. M., Vila-Guerau de Arellano, J., and van Lipzig, N. P. M.: The impact of weather and atmospheric circulation on $O_3$ and $PM_{10}$ levels at a rural mid-latitude site, Atmos. Chem. Phys., 9, 2695–2714, doi:10.5194/acp-9-2695-2009, 2009.

Doherty, R. M., Wild, O., Shindell, D. T., Zeng, G., MacKenzie, I. A., Collins, W. J., Fiore, A. M., Stevenson, D. S., Dentener, F. J., Schultz, M. G., Hess, P., Derwent, R. G., and Keating, T. J.: Impacts of climate change on surface ozone and intercontinental ozone pollution: A multi-model study, J. Geophys. Res.-Atmos., 118, 3744–3763, 2013.

Emberson, L., Simpson, D., Tuovinen, J. P., Ashmore, M., and Cambridge, H. M.: Towards a model of ozone deposition and stomatal uptake over Europe. EMEP MSC-W Note 6/2000. Norwegian Meteorological Institute, Oslo, Norway. (available at: www.emep.int), 2000a.

Emberson, L. D., Ashmore, M. R., Cambridge, H. M., Simpson, D., and Tuovinen, J. P.: Modelling stomatal ozone flux across Europe, Environ. Pollut., 109, 403–413, 2000b.

Engardt, M., Bergström, R., and Andersson, C.: Climate and emission changes contributing to changes in near-surface ozone in Europe over the coming decades - Results from model studies, Ambio, 38, 452–458, 2009.

EU directive 2008/50/EC of the European parliament and of the council on Ambient Air Quality and Cleaner Air for Europe, 21 May 2008.

Fuhrer, J.: Ozone risk for crops and pastures in present and future climates, Naturwissenschaften, 96, 173–194, 2009.

Fuhrer, J., Skärby, L., and Ashmore, M. R.: Critical levels for ozone effects on vegetation in Europe, Environ. Pollut., 97, 91–106, 1997.

Hollaway, M. J., Arnold, S. R., Challinor, A. J., and Emberson, L. D.: Intercontinental trans-boundary contributions to ozone-induced crop yield losses in the Northern Hemisphere, Biogeosciences, 9, 271–292, doi:10.5194/bg-9-271-2012, 2012.

Jarvis, P. G.: The interpretation of the variations in leaf water potential and stomatal conductance found in canopies in the field, Philos. T. Roy. Soc. Lond. B, 87, 593–610, 1976.

Karlsson, P. E., Örlander, G., Langvall, O., Uddling, J., Hjorth, U., Wiklander, K., Areskoug, B., and Grennfelt, P.: Negative impact of ozone on the stem basal area increment of mature Norway spruce in south Sweden, Forest Ecol. Manag., 232, 146–151, 2006.

Karlsson, P. E., Tang, L., Sundberg, J., Chen, D., Lindskog, A., and Pleijel, H.: Increasing risk for negative ozone impacts on vegetation in northern Sweden, Environ. Pollut., 150, 96–106, 2007.

Kjellström, E., Nikulin, G., Hansson, U., Strandberg, G., and Ullerstig, A.: 21st century changes in the European climate: uncertainties derived from an ensemble of regional climate model simulations, Tellus A, 63, 24–40, 2011.

Klingberg, J., Björkman, M. P., Pihl Karlsson, G., and Pleijel, H.: Observations of ground-level ozone and $NO_2$ in northernmost Sweden, including the Scandian Mountain Range Ambio, 38, 448–451, 2009.

Klingberg, J., Engardt, M., Uddling, J., Karlsson, P. E., and Pleijel, H.: Ozone risk for vegetation in the future climate of Europe based on stomatal ozone uptake calculations, Tellus A, 63, 174–187, 2011.

Klingberg, J., Karlsson, P. E., Pihl Karlsson, G., Hu, Y., Chen, D., and Pleijel, H.: Variation in ozone exposure in the landscape of southern Sweden with consideration of topography and coastal climate, Atmos. Environ., 47, 252–260, 2012.

Kolari, P., Lappalainen, H. K., Hanninen, H., and Hari, P.: Relationship between temperature and the seasonal course of photosynthesis in Scots pine at northern timberline and in southern boreal zone, Tellus B, 59, 542–552, 2007.

Langner, J., Engardt, M., and Andersson, C.: European summer surface ozone 1990–2100, Atmos. Chem. Phys., 12, 10097–10105, doi:10.5194/acp-12-10097-2012, 2012a.

Langner, J., Engardt, M., Baklanov, A., Christensen, J. H., Gauss, M., Geels, C., Hedegaard, G. B., Nuterman, R., Simpson, D., Soares, J., Sofiev, M., Wind, P., and Zakey, A.: A multi-model study of impacts of climate change on surface ozone in Europe, Atmos. Chem. Phys., 12, 10423–10440, doi:10.5194/acp-12-10423-2012, 2012b.

Mills, G., Buse, A., Gimeno, B., Bermejo, V., Holland, M., Emberson, L., and Pleijel, H.: A synthesis of AOT40-based response functions and critical levels of ozone for agricultural and horticultural crops, Atmos. Environ., 41, 2630–2643, 2007.

Mills, G., Hayes, F., Simpson, D., Emberson, L., Norris, D., Harmens, H., and Buker, P.: Evidence of widespread effects of ozone on crops and (semi-)natural vegetation in Europe (1990–2006) in relation to AOT40-and flux-based risk maps, Glob. Change Biol., 17, 592–613, 2011.

Monteith, J. and Unsworth, M. H.: Principles of Environmental Physics, 3rd Edn., Academic Press, London, 418 pp., 2008.

Moss, R. H., Edmonds, J. A., Hibbard, K. A., Manning, M. R., Rose, S. K., van Vuuren, D. P., Carter, T. R., Emori, S., Kainuma, M., Kram, T., Meehl, G. A., Mitchell, J. F. B., Nakićenović, N., Riahi, K., Smith, S. J., Stouffer, R. J., Thomson, A. M., Weyant, J. P., and Wilbanks, T. J.: The next generation of scenarios for climate change research and assessment, Nature, 463, 747–756, 2010.

Nakićenović, N., Alcamo, J., Davis, G., Vries, B. d., Fenhann, J., Gaffin, S., Gregory, K., Grobler, A., Jung, T. Y., Kram, T., Rovere, E. L. L., Michaelis, L., Mori, S., Morita, T., Pepper, W., Pitcher, H., Price, L., Riahi, K., Roehrl, A., Rogner, H.-H., Sankovski, A., Schlesinger, M., Shukla, P., Smith, S., Swart, R., Rooijen, S. v., Victor, N., and Dadi, Z.: Emission scenarios. A special report of IPCC Working Group III, Cambridge University Press, 599 pp., 2000.

Paoletti, E.: Ozone and Mediterranean ecology: Plants, people, problems, Environ. Pollut., 157, 1397–1398, 2009.

Pleijel, H.: Reduced ozone by air filtration consistently improved grain yield in wheat, Environ. Pollut., 159, 897–902, 2011.

Pleijel, H., Danielsson, H., Emberson, L., Ashmore, M. R., and Mills, G.: Ozone risk assessment for agricultural crops in Europe: Further development of stomatal flux and flux-response relationships for European wheat and potato, Atmos. Environ., 41, 3002–3040, 2007.

Pleijel, H., Klingberg, J., Karlsson, G. P., Engardt, M., and Karlsson, P. E.: Surface ozone in the marine environment – horizontal ozone concentration gradients in coastal areas, Water Air Soil Poll., 224, 1603,doi:10.1007/s11270-013-1603-4, 2013.

Rafaj, P., Schopp, W., Russ, P., Heyes, C., and Amann, M.: Co-benefits of post-2012 global climate mitigation policies, Mitig. Adapt. Strateg. Glob. Change, 18, 801–824, 2013.

Robertson, L., Langner, J., and Engardt, M.: An Eulerian limited-area atmospheric transport model, J. Appl. Meteorol., 38, 190–210, 1999.

Roeckner, E., Brokopf, R., Esch, M., Giorgetta, M., Hagemann, S., Kornblueh, L., Manzini, E., Schlese, U., and Schulzweida, U.: Sensitivity of simulated climate to horizontal and vertical resolution in the ECHAM5 atmosphere model, J. Climate, 19, 3771–3791, 2006.

Rogel, J., Meinshausen, M., and Knutti, R.: Global warming under old and new scenarios using IPCC climate sensitivity range estimates, Nature Climate Change, 2, 248–253, 2012.

Royal Society: Ground-level ozone in the 21st century: future trends, impacts and policy implications, RS Policy document 15/08, London (available at http://royalsociety.org), 133 pp., 2008.

Samuelsson, P., Jones, C. G., Willen, U., Ullerstig, A., Gollvik, S., Hansson, U., Jansson, C., Kjellstrom, E., Nikulin, G., and Wyser, K.: The Rossby Centre Regional Climate model RCA3: model description and performance, Tellus A, 63, 4–23, 2011.

Sakalli, A. and Simpson, D.: Towards the use of dynamic growing seasons in a chemical transport model, Biogeosciences, 9, 5161–5179, doi:10.5194/bg-9-5161-2012, 2012.

Sandelius, A., Naslund, K., Carlsson, A., Pleijel, H., and Sellden, G.: Exposure of spring wheat (*Triticum aestivum*) to ozone in open-top chambers. Effects on acyl lipid composition and chlorophyll content of flag leaves, New Phytol., 131, 231–239, 1995.

Sitch, S., Cox, P. M., Collins, W. J., and Huntingford, C.: Indirect radiative forcing of climate change through ozone effects on the land-carbon sink, Nature, 448, 791–794, 2007.

Sofiev, M. and Tuovinen, J. P.: Factors determining the robustness of AOT40 and other ozone exposure indices, Atmos. Environ., 35, 3521–3528, 2001.

Tanja, S., Berninger, F., Vesala, T., Markkanen, T., Hari, P., Makela, A., Ilvesniemi, H., Hanninen, H., Nikinmaa, E., Huttula, T., Laurila, T., Aurela, M., Grelle, A., Lindroth, A., Arneth, A., Shibistova, O., and Lloyd, J.: Air temperature triggers the recovery of evergreen boreal forest photosynthesis in spring, Glob. Change Biol., 9, 1410–1426, 2003.

Tank, A., Wijngaard, J. B., Konnen, G. P., Bohm, R., Demaree, G., Gocheva, A., Mileta, M., Pashiardis, S., Hejkrlik, L., Kern-Hansen, C., Heino, R., Bessemoulin, P., Muller-Westermeier, G., Tzanakou, M., Szalai, S., Palsdottir, T., Fitzgerald, D., Rubin, S., Capaldo, M., Maugeri, M., Leitass, A., Bukantis, A., Aberfeld, R., Van Engelen, A. F. V., Forland, E., Mietus, M., Coelho, F., Mares, C., Razuvaev, V., Nieplova, E., Cegnar, T., Lopez, J. A., Dahlstrom, B., Moberg, A., Kirchhofer, W., Ceylan, A., Pachaliuk, O., Alexander, L. V., and Petrovic, P.: Daily dataset of 20th-century surface air temperature and precipitation series for the European Climate Assessment, Int. J. Climatol., 22, 1441–1453, 2002.

Thomson, A. M., Calvin, K. V., Smith, S. J., Kyle, G. P., Volke, A., Patel, P., Delgado-Arias, S., Bond-Lamberty, B., Wise, M. A., Clarke, L. E., and Edmonds, J. A.: RCP4.5: a pathway for stabilization of radiative forcing by 2100, Climatic Change, 109, 77–94, 2011.

Tuovinen, J. P., Emberson, L., and Simpson, D.: Modelling ozone fluxes to forests for risk assessment: status and prospects, Ann. For. Sci., 66, 401, 2009.

Uddling, J., Karlsson, P. E., Glorvigen, A., and Sellden, G.: Ozone impairs autumnal resorption of nitrogen from birch (*Betula pendula*) leaves, causing an increase in whole-tree nitrogen loss through litter fall, Tree Physiol., 26, 113–120, 2006.

Wild, O., Fiore, A. M., Shindell, D. T., Doherty, R. M., Collins, W. J., Dentener, F. J., Schultz, M. G., Gong, S., MacKenzie, I.

A., Zeng, G., Hess, P., Duncan, B. N., Bergmann, D. J., Szopa, S., Jonson, J. E., Keating, T. J., and Zuber, A.: Modelling future changes in surface ozone: a parameterized approach, Atmos. Chem. Phys., 12, 2037–2054, doi:10.5194/acp-12-2037-2012, 2012.

Wittig, V. E., Ainsworth, E. A., Naidu, S. L., Karnosky, D. F., and Long, S. P.: Quantifying the impact of current and future tropospheric ozone on tree biomass, growth, physiology and biochemistry: a quantitative meta-analysis, Glob. Change Biol., 15, 396–424, 2009.

Young, P. J., Archibald, A. T., Bowman, K. W., Lamarque, J.-F., Naik, V., Stevenson, D. S., Tilmes, S., Voulgarakis, A., Wild, O., Bergmann, D., Cameron-Smith, P., Cionni, I., Collins, W. J., Dalsøren, S. B., Doherty, R. M., Eyring, V., Faluvegi, G., Horowitz, L. W., Josse, B., Lee, Y. H., MacKenzie, I. A., Nagashima, T., Plummer, D. A., Righi, M., Rumbold, S. T., Skeie, R. B., Shindell, D. T., Strode, S. A., Sudo, K., Szopa, S., and Zeng, G.: Pre-industrial to end 21st century projections of tropospheric ozone from the Atmospheric Chemistry and Climate Model Intercomparison Project (ACCMIP), Atmos. Chem. Phys., 13, 2063–2090, doi:10.5194/acp-13-2063-2013, 2013.